



Amblyomin-X, a recombinant Kunitz-type inhibitor, regulates cell adhesion and migration of human tumor cells

Mariana Costa Braga Schmidt , Katia L.P. Morais , Máira Estanislau Soares de Almeida , Asif Iqbal , Mauricio Barbugiani Goldfeder & Ana Marisa Chudzinski-Tavassi

To cite this article: Mariana Costa Braga Schmidt , Katia L.P. Morais , Máira Estanislau Soares de Almeida , Asif Iqbal , Mauricio Barbugiani Goldfeder & Ana Marisa Chudzinski-Tavassi (2020) Amblyomin-X, a recombinant Kunitz-type inhibitor, regulates cell adhesion and migration of human tumor cells, Cell Adhesion & Migration, 14:1, 129-138, DOI: [10.1080/19336918.2018.1516982](https://doi.org/10.1080/19336918.2018.1516982)

To link to this article: <https://doi.org/10.1080/19336918.2018.1516982>



© 2020 The Author(s). Published by Informa UK Limited, trading as Taylor & Francis Group



[View supplementary material](#)



Published online: 25 Sep 2018.



[Submit your article to this journal](#)



Article views: 1129



[View related articles](#)



[View Crossmark data](#)



Citing articles: 7 [View citing articles](#)

Amblyomin-X, a recombinant Kunitz-type inhibitor, regulates cell adhesion and migration of human tumor cells

Mariana Costa Braga Schmidt^{a,b}, Katia L.P. Morais^{a,b,c}, Maíra Estanislau Soares de Almeida^{a,c}, Asif Iqbal^{a,c}, Mauricio Barbugiani Goldfeder ^{a,c}, and Ana Marisa Chudzinski-Tavassi^{a,b}

^aLaboratory of Molecular Biology, Butantan Institute, São Paulo, SP, Brazil; ^bDepartment of Biochemistry, Federal University of São Paulo, São Paulo, SP, Brazil; ^cCentre of Excellence in New Target Discovery, Butantan Institute, São Paulo, SP, Brazil

ABSTRACT

In a tumor microenvironment, endothelial cell migration and angiogenesis allow cancer to spread to other organs causing metastasis. Indeed, a number of molecules that are involved in cytoskeleton re-organization and intracellular signaling have been investigated for their effects on tumor cell growth and metastasis. Alongside that, Amblyomin-X, a recombinant Kunitz-type protein, has been shown to reduce metastasis and tumor growth in *in vivo* experiments. In the present report, we provide a mechanistic insight to these antitumor effects, this is, Amblyomin-X modulates Rho-GTPases and uPAR signaling, and reduces the release of MMPs, leading to disruption of the actin cytoskeleton and decreased cell migration of tumor cell lines. Altogether, our data support a role for Amblyomin-X as a novel potential antitumor drug.

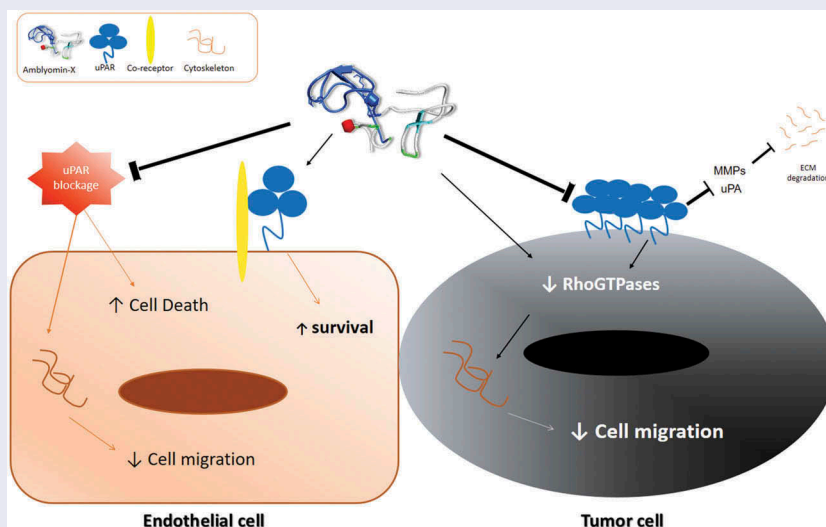
Abbreviations: Amb-X: Amblyomin-X; ECGF: endothelial cell growth factor; ECM: extracellular matrix; GAPDH: glyceraldehyde-3-phosphate dehydrogenase; HUVEC: human umbilical vein endothelial cell; LRP1: low-density lipoprotein receptor-related protein; MMP: matrix metalloproteinase; HPI-4: hedgehog pathway inhibitor 4; PAI-1: plasminogen activator inhibitor 1; PMA: phorbol 12-myristate-13-acetate; TFPI: tissue factor pathway inhibitor; uPA: urokinase plasminogen activator; uPAR: uPA receptor.

ARTICLE HISTORY

Received 2 May 2018
Revised 22 July 2018
Accepted 20 August 2018

KEYWORDS

Amblyomin-X; Kunitz-type inhibitor; cytoskeleton; migration; uPAR; Rho-GTPase




Introduction

Cell migration is a necessary event in many biological processes, including embryo development, angiogenesis, immunological mechanisms, and wound healing [1]. In human pathology, migration of cancer cells

favors metastatic growth to distant organs via lymphatic and blood vessels dissemination [2,3]. Cell migration depends on proteolytic enzymes, receptors and other molecules involved in extracellular matrix (ECM) degradation, rearrangement of cytoskeleton,

CONTACT Ana Marisa Chudzinski-Tavassi  ana.chudzinski@butantan.gov.br  Laboratório de Biologia Molecular, Instituto Butantan - Av. Vital Brasil, 1500, São Paulo, SP 05503-900, Brasil

 Supplemental data for this article can be accessed [here](#).

© 2020 The Author(s). Published by Informa UK Limited, trading as Taylor & Francis Group
This is an Open Access article distributed under the terms of the Creative Commons Attribution-NonCommercial-NoDerivatives License (<http://creativecommons.org/licenses/by-nc-nd/4.0/>), which permits non-commercial re-use, distribution, and reproduction in any medium, provided the original work is properly cited, and is not altered, transformed, or built upon in any way.

cell adhesion and detachment[4]. For this reason, cellular and molecular targets of different migration/invasion systems have been considered as potential new treatment strategies. For instance, tissue factor pathway inhibitor 2 (TFPI-2) has been shown to have antiangiogenic and antitumor properties [5,6] due to its inhibitory properties on serine proteases, matrix metalloproteinases (MMPs), and other molecules involved in the degradation of ECM [7–9]. In a similar fashion, the Kunitz-type inhibitor bikunin was reported to hinder tumor invasion and metastasis by suppressing plasmin activity and expression of urokinase plasminogen activator (uPA) and its receptor (uPAR) [10,11].

Tumor and endothelial cells of the tumor microenvironment express higher amounts of uPAR than normal cells, thus favoring uPA proteolysis and cell migration [12,13]. The uPA/uPAR system induces cell migration through plasmin generation that degrades directly the ECM or by activation of MMPs. However, uPAR may also activate intracellular signaling pathways related to Rho-GTPases, a family of small G proteins (mainly Rho, Rac and Cdc42)[14]. These proteins are involved in transcriptional regulation of many genes, thereby regulating cell size, polarity and mobility[15]. RhoA, for example, is responsible for the induction of focal adhesion, cell contraction, and formation of actin filaments, whereas Cdc42 and Rac induce filopodia and lamellipodia formation, respectively. In addition, uPAR in association with LRP1, integrins, caveolin and vitronectin regulates cytoskeleton reorganization, formation of new focal adhesion and migration [16–19]. Binding of uPA in complex with its inhibitor (plasminogen activator inhibitor 1: PAI-1), can activate intracellular signaling by inducing the internalization of the complex uPA/uPAR/PAI-1/LRP1/integrin [18,20,21]. Therefore, the functional inhibition of uPAR in tumor cells by Kunitz-type inhibitors may regulate cell cytoskeleton and migration, thereby controlling metastasis.

Amblyomin-X is a Kunitz-type inhibitor identified in the transcriptome of the salivary glands from the adult *Amblyomma sculptum* tick. A recombinant form of this protein was shown to have strong proapoptotic activity in various murine and human tumor cells via endoplasmic reticulum stress (ER stress), proteasome inhibition, blockage of autophagy, cell cycle arrest, and aggregates formation [22–24]. *In vivo*, we have shown that this inhibitor induces tumor regression and reduction of metastasis[25]. Furthermore, Amblyomin-X has no toxicity in normal cells and presents low toxicity in healthy animals [22,24,26]. Herein, we demonstrate that

Amblyomin-X alters the formation of the actin cytoskeleton and reduces the migration of tumor cells via modulation of Rho-GTPases and uPAR signaling and reduction of the release of MMPs, giving further insights on its mode of action.

Results

Amblyomin-X reduced the viability and migration of tumor cells

First, the cytotoxic effect of Amblyomin-X upon tumor and normal cells was evaluated. Amblyomin-X treatment considerably decreased the viability of SK-MEL-28 (45.51%) and MIA PaCa-2 (51.50%) as shown in [Figure 1\(a\)](#). In contrast, HUVECs treated with Amblyomin-X remained viable up to 48 h. As expected, bortezomib, staurosporine and MG-132 reduced the viability of all healthy and tumor cell lines tested ([Figure 1\(a\)](#)). In agreement, ERK activation were observed only in HUVECs, but not in human tumor cells (Supplementary Figure 1).

Next, the effect of Amblyomin-X on cytoskeleton organization was investigated and compared to treatment with PMA (phorbol 12-myristate-13-acetate, known to cause changes in the cytoskeleton structure). A mild disorganization of actin filaments was observed in SK-MEL-28 and MIA PaCa-2 after Amblyomin-X treatment ([Figure 1\(b\)](#)) and no alterations were observed in the formation of stress fibers in HUVECs. PMA induced F-actin redistribution and actin epical edge loss mainly in HUVEC and SK-MEL-28 cells. Bortezomib altered the cytoskeletal formation and the morphology of both tumor cells and endothelial cells ([Figure 1\(b\)](#)).

Migration assays in time lapse are presented in [Figure 2](#) and in the supplementary material (Movies S1-S6). In SK-MEL-28, motility was reduced after Amblyomin-X treatment. In this case, an increased amount of cellular extensions was observed (black arrows in [Figure 2](#)), which appeared after longer monitoring times. In addition, cells became thinner and longer (circle in [Figure 2](#) and Supplementary material; Movies S3-S4). MIA PaCa-2 cells are small and have rounder morphology compared to other cell type studied. Its motility profile was already slower than other cells and become even slower when treated with Amblyomin-X. This treatment also induced cells to elongate (black arrow in [Figure 2](#) and Supplementary material; Movie S5-S6).

On the other hand, HUVECs were not affected by Amblyomin-X treatment, presenting large cell membrane movement, large lamellipodia and characteristic motility profile ([Figure 2](#) and Supplementary material; Movies S1-S2).

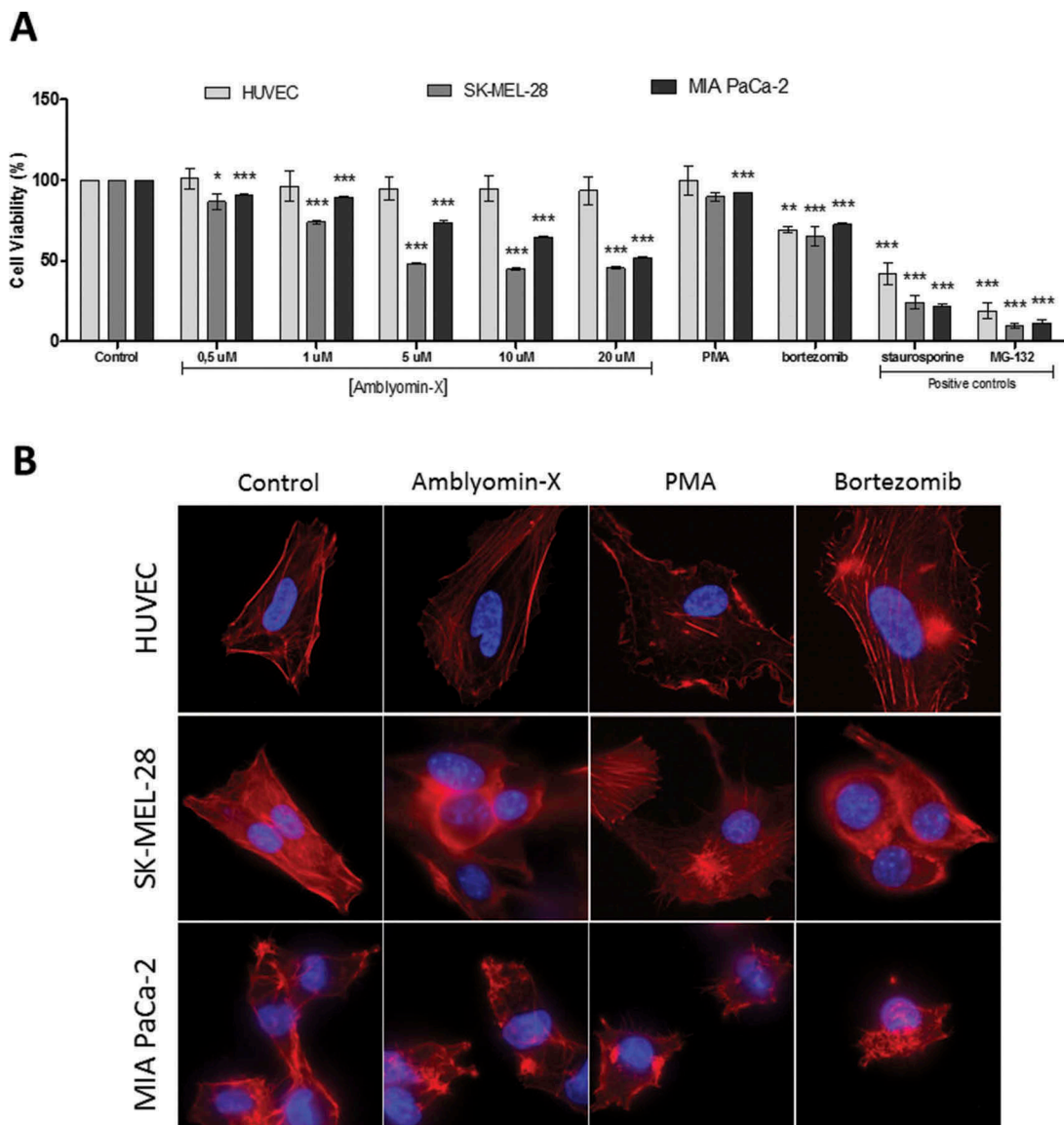


Figure 1. Cytotoxic activity and modulation of the cytoskeleton by Amblyomin-X. (A) All cells types were incubated with Amblyomin-X at the indicated concentrations or PMA (200 nM) and bortezomib (100 nM) for 48 h, and cell viability was assessed as described in Materials and Methods. Positive controls staurosporine (5 μM) and MG-132 (3 μM) were evaluated during the same period of treatment. (B) Representative images of F-actin cytoskeleton of HUVEC, SK-MEL-28 and MIA PaCa-2. After 24 h of treatment with Amblyomin-X (20 μM), PMA (200 nM) or bortezomib (100 nM), cells were fixed and stained. Red represents F-actin labeling with phalloidin and blue represents the nucleus stained with DAPI. Image visualized in 100x, bar 20 μm. Values are mean ± SD of three independent experiments. * $p \leq 0,05$; ** $p \leq 0,01$ e *** $p \leq 0,001$.

Amblyomin-X modulated molecules involved in the regulation of cytoskeleton and cell migration

Comparisons with known molecules that have some similarity (multiple sequence alignment, structure analysis, effects, target, etc.) have been supported many studies to highlighted new targets or pathways. [9–13] Thereby, as many Kunitz-type inhibitors trigger their antitumor and anti-metastatic effects by modulation of uPAR, MMPs and Rho-GTPases, experiments were conducted in order to verify whether Amblyomin-X

effects are associated with these pathways. uPAR-related pathway was investigated with cells previously treated, or co-treated with an anti-uPAR antibody, partially blocking this receptor prior to the treatments.

uPAR-related pathway is involved in the cytotoxic effect of amblyomin-X

Cell viability assays showed that pre-treatment with anti-uPAR reduced Amblyomin-X cytotoxic in SK-MEL-28 cells (Amblyomin-X: 45.51; anti-uPAR + Amblyomin-X: 80.51%), but did not interfere in the reduction of viability

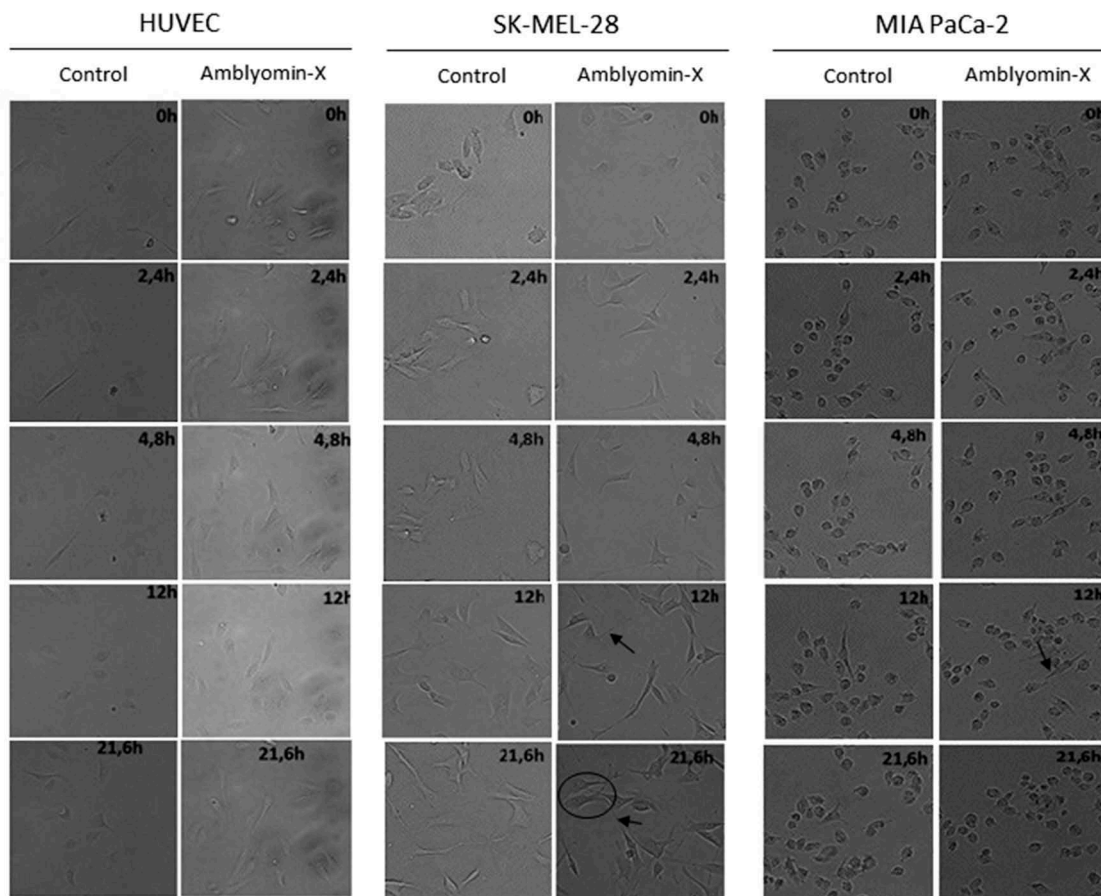


Figure 2. Modulation of cellular migration by Amblyomin-X. Cell migration assays were performed in time lapse (In Cell Analyzer 2200) during 24 hours of treatment with 20 μ M Amblyomin-X. The arrows highlight cell extensions and circles emphasize the change in cell morphology. Movies are available in the supplementary material.

of MIA PaCa-2 cells (Amblyomin-X: 51.5; anti-uPAR + Amblyomin-X: 44.4%). Of note, anti-uPAR treatment promotes a significant reduction of HUVECs viability that was reversed by Amblyomin-X treatment (anti-uPAR: 66.05%; anti-uPAR + Amblyomin-X: 91.42%) (Figure 3(a)).

uPAR-related pathway is associated to cytoskeleton organization and migration profile induced by Amblyomin-X

SK-MEL-28 treated with anti-uPAR displayed pronounced fragmentation of F-actin, which was reverted by Amblyomin-X treatment (Figures 3(b) and 4; Supplementary material, Movie S09-S10). However, we did not observe changes in the morphology and migration profile of MIA PaCa-2 (Figures 3(b) and 4; Supplementary material, Movie S11-S12). Reduction of HUVECs motility by anti-uPAR treatment was rescued by Amblyomin-X (Figures 3(b) and 4; Supplementary material, Movie S7-S8).

Modulation of uPAR and rho-gtpases by Amblyomin-X

Amblyomin-X treatment reduced simultaneously the production of uPAR and small GTPases only in tumor cells (Figure 5). However, the combination with anti-uPAR treatment partially recovered their expression. Similarly, in HUVECs, treatment with Amblyomin-X induced changes in the protein level of uPAR, but it was possible to identify an upper band that may correspond to the complexed form with co-receptors (Figure 5).

PMA and bortezomib showed distinct effect between all cells types.

Regulation of MMPs by Amblyomin-X

Metalloproteinase profiles were evaluated following the same experimental conditions previously described. In SK-MEL-28 cells, Amblyomin-X reduced the amount of MMP-9, but did not alter secretion of MMP-2 (Figure 6). However, when anti-uPAR were co-applied with Amblyomin-X, there was an increase of active MMP-9. In contrast, treatment of MIA PaCa-2 cells with Amblyomin-X induced a decrease of secretion of

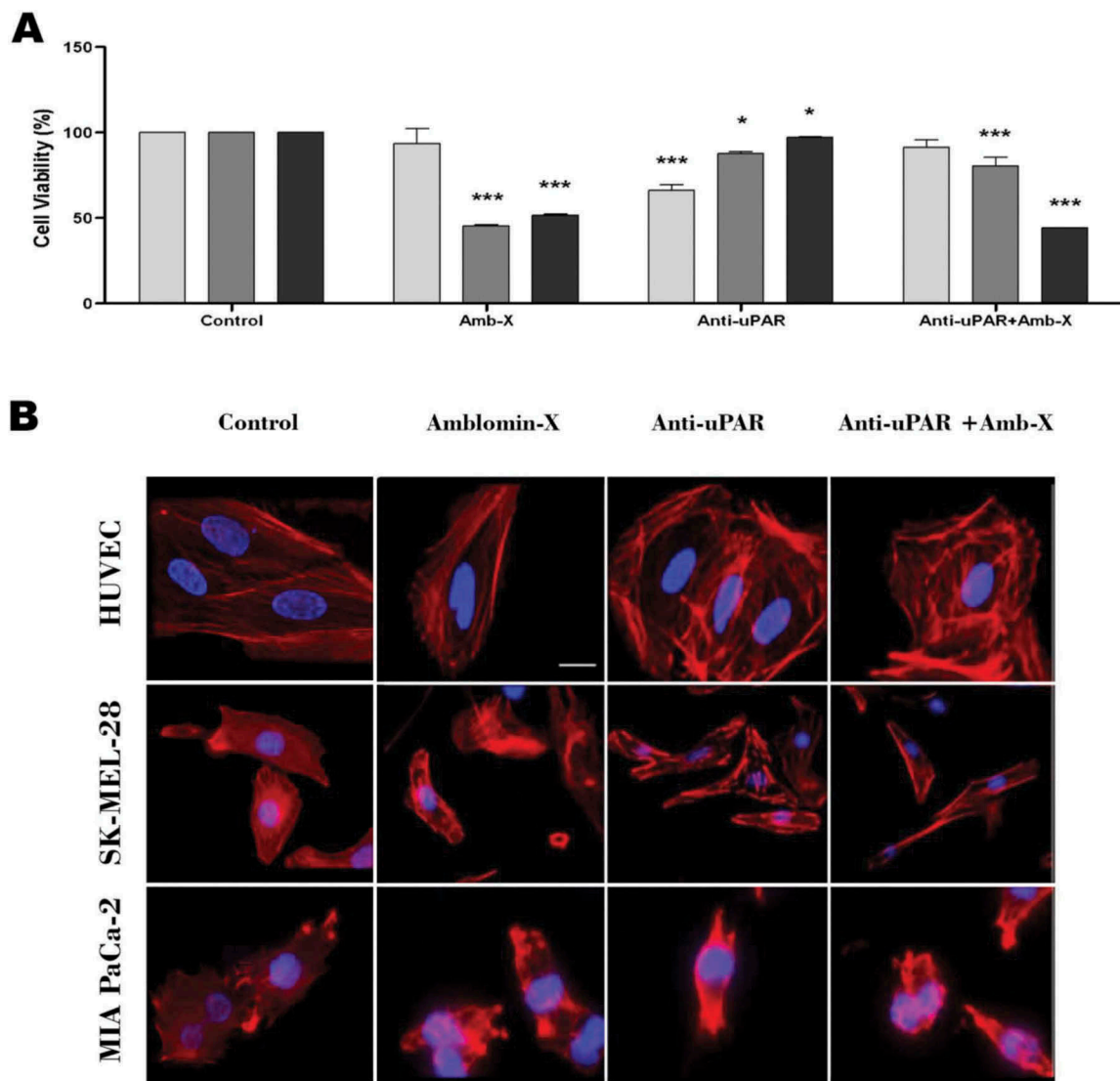


Figure 3. Interference of uPAR blockade in Amblyomin-X activity. All cell types were treated with anti-uPAR 1:50 (30 min), followed by treatment with 20 μ M Amblyomin-X. (A) Cell viability measured by MTT (48 h of treatment). (B) Representative image of F-actin cytoskeleton of HUVEC, SK-MEL-28 and MIA PaCa-2 (24 h of treatment). Red represents F-actin stained with phalloidin and blue represents the nucleus stained with DAPI. Bar 20 μ m. Values are mean \pm SD of three independent experiments. * $p \leq 0,05$; ** $p \leq 0,01$ e *** $p \leq 0,001$. Significance was compared among treated and control (untreated cells) or between the couple of treatments (not shown).

MMP-2 and MMP-9. In HUVECs, we observed that treatment with Amblyomin-X induced only a reduction in MMP-2 levels, but did not affect MMP-9 (Figure 6).

PMA treatment caused a slight increase in both MMPs in MIA PaCa-2 and HUVECs, while bortezomib increased those MMPs only in both tumor cells.

Discussion

The current study describes cellular effects induced by Kunitz-type inhibitor associated with distinct cell motility and proteolysis pericellular biological processes in tumor and endothelial cells. We have demonstrated before that

Amblyomin-X has antitumor, antithrombotic and anti-metastatic activity [25–28]. Interestingly, no cytotoxic effect was reported in non-tumor cells, such as fibroblasts. Previously, we have reported that reduction of cell viability induced by Amblyomin-X is associated with proapoptotic stimuli induced by Amblyomin-X, i.e. proteasome inhibition, endoplasmic reticulum stress, cell cycle disruption, mitochondrial dysfunction and caspase activation [22,26,29]. Herein, we have demonstrated that Amblyomin-X reduces cell viability of tumor cells, in agreement to our previous reports, and show for the first time its involvement on the motility reduction and cytoskeletal disorganization. Notably, Amblyomin-X did

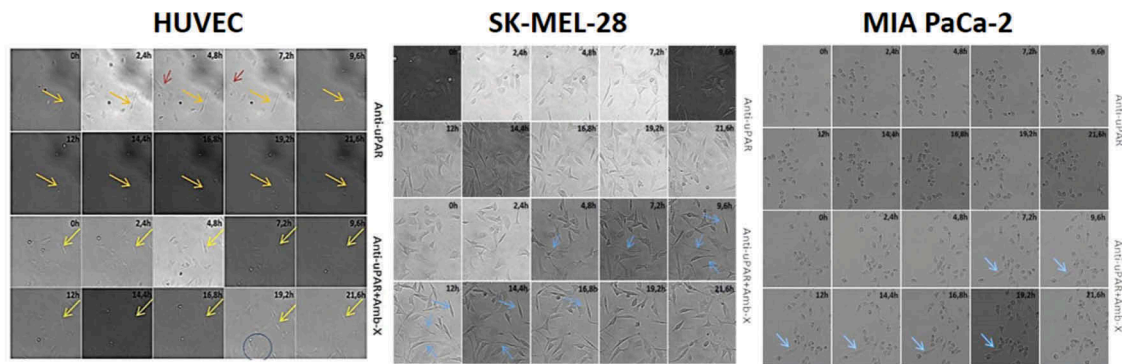


Figure 4. Analysis of Amblyomin-X activity in the migration of cells subjected to uPAR blockade. Cells were incubated with anti-uPAR 1:50 (30 min), followed add of Amblyomin-X (20 μ M). The arrows highlight cell extensions and circles emphasize the change in cell morphology. Movies are available in the supplementary material.

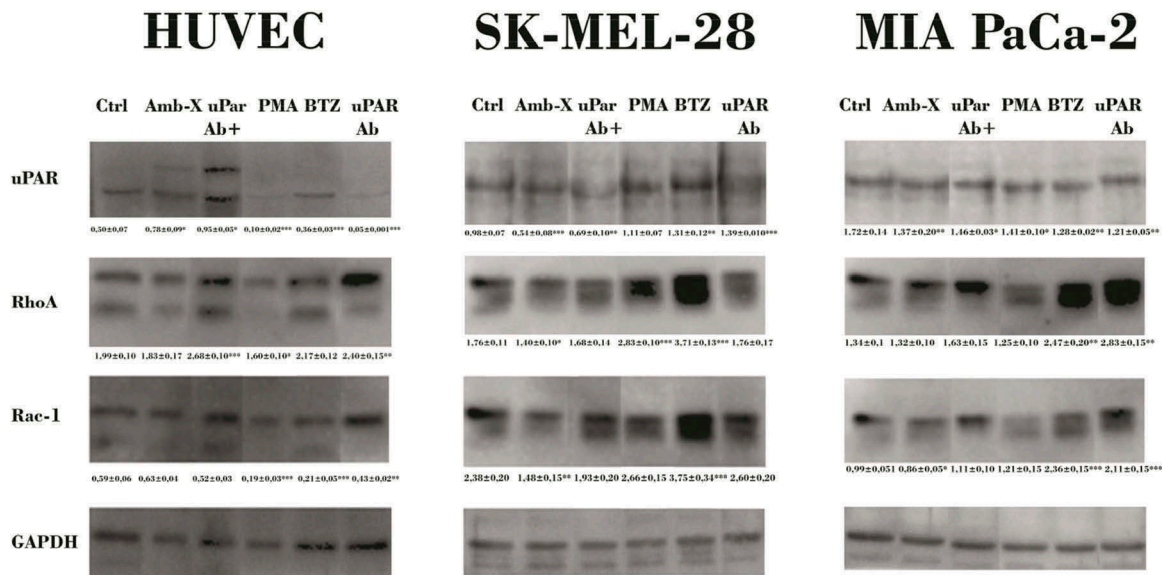


Figure 5. Reduction Rho GTPases protein levels by Amblyomin-X. Cells were treated with anti-uPAR 1:50 (30 min), followed by incubation with 20 μ M Amblyomin-X (24 h). Treatments with 200 nM PMA or 100 nM bortezomib for 24 h were used as comparative. After the treatment period, cells were lysed with RIPA buffer and 30 μ g of total protein was used for the assays. Western blot of the samples obtained were performed using anti-uPAR, anti-RhoA, anti-Rac-1 and anti-GAPDH antibodies as endogenous control (see experimental procedures). Densitometry analysis of protein bands (numbers below the figures) were evaluate using ImageJ analysis program and values are mean \pm SD of three independent experiments. Significance was compared among the treated and control (untreated cells) or between the couple of treatments (not shown). uPar Ab+: co-treatment with Amblyomin-X.

not alter the viability, organization of cytoskeleton or cell motility of HUVECs. Therefore, our findings differentiate Amblyomin-X from other Kunitz-type inhibitors such as TFPI-1 and TFPI-2, which inhibit proliferation, migration and adhesion in both tumor and normal endothelial cells, [10,11,30,31] this is, lack specificity for tumor cells, unlike Amblyomin-X.

Many Kunitz-type inhibitors regulates uPA and uPAR [10,11], which are involved in several biological processes, such as actin filament formation, migration and cell adhesion [13,19]. Therefore, we investigated the effect of Amblyomin-X in uPAR signaling. In human melanoma cells (SK-MEL-28), pretreatment

with anti-uPAR reduced the cytotoxic effect of Amblyomin-X. Interestingly, Amblyomin-X reduced the modification of the actin filaments caused by the anti-uPAR. Also, Amblyomin-X slightly decreased the protein levels of RhoA and Rac-1, which could be associated with cytoskeletal modifications and inhibition of migration. Previously, we have reported that Amblyomin-X leads the connection Rho-GEF to dynein or, in other words, its inactivation. [24]

Furthermore, in MIA PaCa-2 cells, blocking of uPAR did not affect the cytotoxic activity, cytoskeletal disorganization or cell migration inhibition promoted by Amblyomin-X. However, we observed reduction of

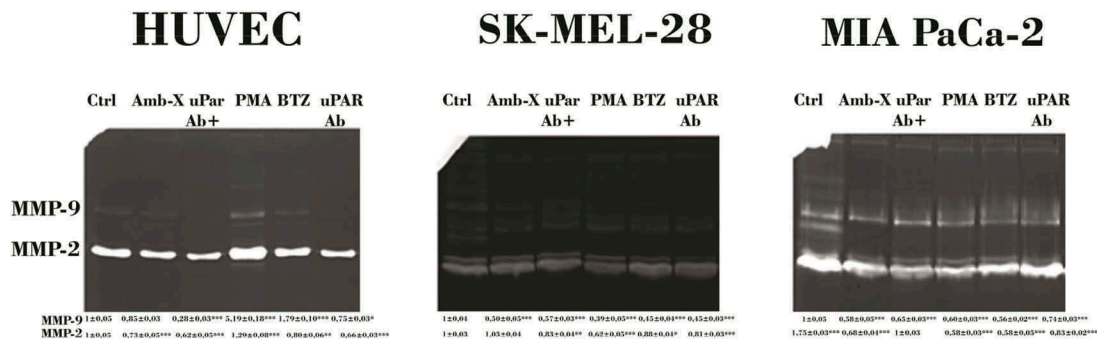


Figure 6. Modulation of MMPs release by Amblyomin-X. All cell types were preincubated 30 min with anti-uPAR (1:50), followed by incubation with Amblyomin-X (20 μ M) for 24 h at 37°C. PMA (200 nM) and bortezomib (100 nM) for 24 h were also evaluated. After the treatment period, the cell supernatants collected were submitted to the zymography test as discussed in experimental procedures. Densitometry analysis of protein bands (numbers below the figures) were evaluated using ImageJ analysis program and values are mean \pm SD of three independent experiments. Significance was compared among treated and control (untreated cells) or between the couple of treatments (not shown).

uPAR and Rho-GTPases protein levels as well as reversion of all the changes promoted by anti-uPAR in Rho-GTPases levels. Thereby, similar to melanoma cells, Amblyomin-X modulates these pathways, but further signaling is needed to induce viability reduction and cell migration induced in this cell type.

Interestingly, endothelial cells are not affected by Amblyomin-X. In contrast, this molecule reduced effects induced by anti-uPAR (cytotoxic, cell migration inhibition and Rac-1 reduction) and induced complexation of uPAR with co-receptors as shown in immunoblot experiments in HUVECs. Taken all these results together, we hypothesized that the complexed form of uPAR is associated with survival pathways.

Overall, we observed significantly reduced levels of the activated MMP-9 in tumor cell lines (MIA PaCa-2 and SK-MEL-28) treated with Amblyomin-X compared to their corresponding controls. Such type of effect on MMP9 was not observed in HUVECs treated with Amblyomin-X. Somehow, in both tumor cells Amblyomin-X altered the protein levels and uPAR activity and it was supported by reduced levels MMP-9 (MMPs are activated via uPAR-uPA \rightarrow plasmin \rightarrow MMP). These findings further strengthen our concept of Amblyomin-X influence on uPAR signaling. Also, all differences when Amblyomin-X and anti-uPAR were co-treated suggest that Amblyomin-X acts synergistically with inhibitor to modulated transmembrane partner, signaling and regulators of uPAR in all cell types.

Considering all these findings, it is relevant to mention that Amblyomin-X is not a trypsin inhibitor. Indeed, this molecule is a substrate for plasmin and trypsin. [27] Also, as suggested previously Amblyomin-X is different from Kunitz-type inhibitors that bind to

the active site and strongly inhibit serine proteases. Probably it binds to an exosite of factor Xa and this might be the reason why Amblyomin-X functions as a noncompetitive inhibitor for factor Xa and a substrate for trypsin and plasmin. Thereby, we believe that uPA/uPAR signaling modulation by Amblyomin-X is different from others Kunitz-type inhibitors, for example, with no suppression ERK in human tumor cells (supplementary Figure 1) as shown for bikunin. [32] Thus, Amblyomin-X studies could bring new findings regarding uPAR signalling regulation, as well as selectivity for tumor cells.

Finally, all results present in this study shown that Amblyomin-X and bortezomib act distinctively. Bortezomib is used as chemotherapeutic in the treatment of different types of cancer, but its effects are not restricted to tumor cells and triggers several side effects [33–36]. Indeed, in our experiments we observed that bortezomib induced: (i) cytotoxicity and cytoskeleton disorganization of both tumor cells and endothelial cells; (ii) modulates MMPs in all cell types; (iii) increased RhoA in HUVECs, SK-MEL-28 and MIA PaCa-2 cells, which could facilitate the metastasis and tumor angiogenesis during cancer treatment [37–39]. On the other hand Amblyomin-X induces death specifically in tumor cells, preserves endothelial cells i.e. do not affect normal cells and reverts many effects of uPAR blockage, which are indeed highly valued advantages of this molecule over bortezomib.

In conclusion, we demonstrate an additional novel mechanism for Amblyomin-X for the control tumor cell growth and metastasis, i.e., modulation uPAR signaling and Rho-GTPase and reduces the release of MMPs, leading to disruption of the actin cytoskeleton and decreased cell migration. Notably, negligible effect

in HUVECs and protection from disturbances on cytoskeleton and migration, suggest that Amblyomin-X may be a potential safety antitumor and open new avenues in cell motility and proteolysis pericellular.

Materials and methods

Amblyomin-X production

Recombinant Amblyomin-X was expressed and purified from *E. coli*, as reported elsewhere[40].

Cell lines and culture conditions

Human melanoma (SK-MEL-28) and pancreatic adenocarcinoma (MIA PaCa-2) cells were obtained and cultured according to instructions from the American Type Culture Collection (ATCC, Manassas, VA). Endothelial cells were obtained from human umbilical veins (HUVECs), as previously described[41], with a few modifications. The study received prior approval from Ethics Committee in Research of Heliopolis Hospital, São Paulo, Brazil (CAAE 48,984,915.3.0000.5449, NUMBER 1.404.230) and written informed consent was obtained from women donors. HUVECs were seeded onto T75 flasks previously covered with 2% gelatin and were grown in RPMI, supplemented with 10% fetal bovine serum, L-glutamine (2 mM), streptomycin sulfate (100 mg/ml), penicillin (100 U/ml), sodium pyruvate (100 mM), 2-mercaptoethanol (10 mM), ECGF (10 mg/mL) and heparin (45 µg/mL), pH 7.4. In all experiments, HUVECs were used in second or third passage. All cell types were routinely grown in a humidified 5% CO₂ incubator at 37°C.

Cell viability

Cell viability was measured by MTT assay as described elsewhere [24]. In order to investigate uPAR signaling, HUVECs and SK-MEL-28 and Mia-PaCa-2 cells were seeded in 96-well plates (10 [4] cells/well) and pre-incubated with an anti-uPAR antibody (10 µM) for 30 min. Bortezomib (100 nM) and PMA (200 nM) were used for comparative purpose. Beside, staurosporine (5 µM) and MG-132 (3 µM) were used as positive control.

F-actin visualization by fluorescence microscopy

After treatments, cells were fixed and permeabilized in PHEM-glycine buffer (2mM HEPES, 10 mM EGTA, 2 mM MgCl₂, 60 mM Pipes, 100 mM glycine, pH 6.9) and supplemented with paraformaldehyde (4%), Triton

X-100 (0.25%) and sucrose (146 mM) for 15 min. Then, Rhodamine-conjugated phalloidin (Invitrogen, USA) was used to stain actin filaments. Cells were washed with PHEM-glycine buffer before imaging and cell nuclei was stained with DAPI in Vectashield mounting medium (Vector Labs, USA). Fluorescence signals were imaged using an Olympus BX51 inverted fluorescent microscope using appropriate filters.

Real-time cell analysis

To analyze cell migration, a real-time assay was performed using InCell-Analyzer 2200 (GE, EUA). Briefly, cells were grown in 24-well plates until approximately 30% confluence. Cells were then treated with Amblyomin-X (20 µM) for 2 h, followed by 24 h incubation in the cell analyzer equipment. The images were acquired with 40x objective and analyzed using the InCell Investigator software V1.6.1 (GE, USA). Bortezomib (100 nM) and PMA (200 nM) were used as controls. Also, to investigate uPAR signaling, cells were pre-incubated with an anti-uPAR antibody (10 µM) for 30 min.

Zymography of cell supernatants

Proteins in cell supernatants (30 µL) from HUVECs, SK-MEL-28 and MIA PaCa-2 cells treated as previously described in the absence of fetal bovine serum, were separated on 15% SDS-PAGE containing 0.1% gelatin in the separating gel[42]. Gels were carefully transferred to 100 mL of renaturing solution (2.5% v/v Triton X-100 in water) and incubate for 30 min at room temperature with gentle agitation. The gels were washed twice with 300 mL of water and gels were incubate at room temperature in 100 mL of developing buffer (50 mM Tris-HCl, pH 7.8, 200mM NaCl, 5 mM CaCl₂ and 0.2%) with gentle agitation. After 30 min, fresh developing buffer was added and the gels were incubated overnight at 37°C. The developing buffer was decanted and the gels were stained for 1h with Commassie blue staining. Gels were then destained in 10% ethanol and 5% acetic acid until clear bands of gelatinolytic activity appeared over the blue background. ImageJ software (National Institute of Health, USA) was used for quantification of the bands.

Western blot analysis

HUVEC, SK-MEL-28 and MIA PaCa-2 were treated as described previously for 24h. Cells lysates were obtained with RIPA buffer (1% deoxycholate, 150 mM NaCl, 1% SDS, 10 mM NaF, 1% TritonX-100, 50 mM Tris-HCl,

2 µg/mL aprotinin, 1 mM PMSF, 1 mM orthovanadate) and submitted to 15% SDS-PAGE. Proteins were transferred onto nitrocellulose membranes, which were blocked for 2 h with TBST containing 1% (w/v) BSA. Membranes were incubated with primary antibodies (1:2500) in TBST containing 0.1% (w/v) BSA for 2 h and with secondary antibodies for 1 hour (1:5000; conjugated with horseradish peroxidase), following development with ECL substrate. Primary antibodies against anti-uPAR, anti-RhoA, and anti-GADPH were purchased from Santa Cruz Biotechnology Inc. (TX, USA) and anti-Rac-1 was purchased from Abcam (CAM, RU). ImageJ suite (National Institute of Health, USA) was used for quantification of the bands.

Statistical analysis

Comparisons were carried out by using Two-way ANOVA analysis followed by Tukey's Post Hoc test or tTest, employing the GraphPad Prism 5.0 software (GraphPad Software Inc., San Diego, CA). The criteria for statistical significance were set up as * $p \leq 0.05$; ** $p \leq 0.01$ and *** $p \leq 0.001$.

Acknowledgments

This study was supported by grants provided by the São Paulo Research Foundation (FAPESP; processes 2014/24512-3, CETICs 2013/07467-1 and 2015/50040-4, São Paulo Research Foundation and GlaxoSmithKline). The authors thank the National Counsel of Technological and Scientific Development (CNPq, INCTTox), Coordination of Improvement of Higher Education Personnel (CAPES), BNDES 13.2.0711.1/2013 and União Química Farmacêutica Nacional for the support.

We also acknowledge Dr. Sergio Cavalheiro, pediatric neurosurgeon at the Santa Paula Hospital in São Paulo and Dr. Carlos de Ocesano Pereira for helpful discussions. We are grateful to the technician Ivan Novaski, from Laboratory of Cell Cycle (Cetics/Cepid) from Butantan Institute. We thank Prof. Eduardo Angles-Cano from INSERM UMR_S 1140-Université Paris Descartes, Sorbonne Paris Cité for discussions and critical reading of the manuscript.

Disclosure statement


No potential conflict of interest was reported by the authors.

Funding

This work was supported by the Fundação de Amparo à Pesquisa do Estado de São Paulo [2015/50040-4]; Fundação de Amparo à Pesquisa do Estado de São Paulo [2013/07467-1]; Fundação de Amparo à Pesquisa do Estado de São Paulo [2014/24512-3]; National Counsel of Technological and Scientific Development (CNPq, 305445/2013-8) [N/A]; Coordination of Improvement of Higher Education Personnel (CAPES),

[N/A]; União Química Farmacêutica Nacional [N/A]; BNDES [13.2.0711.1/2013];

ORCID

Mauricio Barbugiani Goldfeder  <http://orcid.org/0000-0001-5115-6775>

References

- [1] Yamaguchi H, Condeelis J. Regulation of the actin cytoskeleton in cancer cell migration and invasion. *Biochim Biophys Acta.* 2007;1773:642–652.
- [2] Kunigal S, Gondi CS, Gujrati M, et al. SPARC-induced migration of glioblastoma cell lines via uPA-uPAR signaling and activation of small GTPase RhoA. *Int J Oncol.* 2006;29:1349–1357.
- [3] Gutierrez LS, Schulman A, Brito-Robinson T, et al. Tumor development is retarded in mice lacking the gene for urokinase-type plasminogen activator or its inhibitor, plasminogen activator inhibitor-1. *Cancer Res.* 2000;60:5839–5847.
- [4] Salamone M, Carfi Pavia F, Gherzi G. Proteolytic enzymes clustered in specialized plasma-membrane domains drive endothelial cells' migration. *PloS one.* 2016;11:e0154709.
- [5] Chand HS, Foster DC, Kisiel W. Structure, function and biology of tissue factor pathway inhibitor-2. *Thromb Haemost.* 2005;94:1122–1130.
- [6] Izumi H, Takahashi C, Oh J, et al. Tissue factor pathway inhibitor-2 suppresses the production of active matrix metalloproteinase-2 and is down-regulated in cells harboring activated ras oncogenes. *FEBS Lett.* 2000;481:31–36.
- [7] Kondraganti S, Gondi CS, Gujrati M, et al. Restoration of tissue factor pathway inhibitor inhibits invasion and tumor growth in vitro and in vivo in a malignant meningioma cell line. *Int J Oncol.* 2006;29:25–32.
- [8] Tang Z, Geng G, Huang Q, et al. Expression of tissue factor pathway inhibitor 2 in human pancreatic carcinoma and its effect on tumor growth, invasion, and migration in vitro and in vivo. *J Surg Res.* 2011;167:62–69.
- [9] Williams L, Tucker TA, Koenig K, et al. Tissue factor pathway inhibitor attenuates the progression of malignant pleural mesothelioma in nude mice. *Am J Respir Cell Mol Biol.* 2012;46:173–179.
- [10] Kobayashi H, Yagyu T, Inagaki K, et al. Bikunin plus paclitaxel markedly reduces tumor burden and ascites in mouse model of ovarian cancer. *Int J Cancer.* 2004;110:134–139.
- [11] Bayraktar E, Igci M, Erturhan S, et al. Reduced gene expression of bikunin as a prognostic marker for renal cell carcinoma. *Exp Oncol.* 2014;36:107–111.
- [12] Muller SM, Okan E, Jones P. Regulation of urokinase receptor transcription by Ras- and Rho-family GTPases. *Biochem Biophys Res Commun.* 2000;270:892–898.
- [13] Smith HW, Marshall CJ. Regulation of cell signalling by uPAR. *Nat Rev Mol Cell Biol.* 2010;11:23–36.
- [14] Hall A. Rho family GTPases. *Biochem Soc Trans.* 2012;40:1378–1382.

- [15] Gerthoffer WT. Mechanisms of vascular smooth muscle cell migration. *Circ Res.* 2007;100:607–621.
- [16] Margheri F, Luciani C, Taddei ML, et al. The receptor for urokinase-plasminogen activator (uPAR) controls plasticity of cancer cell movement in mesenchymal and amoeboid migration style. *Oncotarget.* 2014;5:1538–1553.
- [17] Balsara RD, Merryman R, Virjee F, et al. A deficiency of uPAR alters endothelial angiogenic function and cell morphology. *Vasc Cell.* 2011;3:10.
- [18] Duffy MJ, Duggan C. The urokinase plasminogen activator system: a rich source of tumour markers for the individualised management of patients with cancer. *Clin Biochem.* 2004;37:541–548.
- [19] Degryse B, Resnati M, Rabbani SA, et al. Src-dependence and pertussis-toxin sensitivity of urokinase receptor-dependent chemotaxis and cytoskeleton reorganization in rat smooth muscle cells. *Blood.* 1999;94:649–662.
- [20] Sid B, Dedieu S, Delorme N, et al. Human thyroid carcinoma cell invasion is controlled by the low density lipoprotein receptor-related protein-mediated clearance of urokinase plasminogen activator. *Int J Biochem Cell Biol.* 2006;38:1729–1740.
- [21] Czekay RP, Wilkins-Port CE, Higgins SP, et al. PAI-1: an integrator of cell signaling and migration. *Int J Cell Biol.* 2011;2011:562481.
- [22] Morais KL, Pacheco MT, Berra CM, et al. Amblyomin-X induces ER stress, mitochondrial dysfunction, and caspase activation in human melanoma and pancreatic tumor cell. *Mol Cell Biochem.* 2016;415:119–131.
- [23] Pacheco MT, Berra CM, Morais KL, et al. Dynein function and protein clearance changes in tumor cells induced by a Kunitz-type molecule, Amblyomin-X. *PLoS one.* 2014;9:e111907.
- [24] Pacheco MT, Morais KL, Berra CM, et al. Specific role of cytoplasmic dynein in the mechanism of action of an antitumor molecule, Amblyomin-X. *Exp Cell Res.* 2016;340:248–258.
- [25] de Souza JG, Morais KL, Angles-Cano E, et al. Promising pharmacological profile of a Kunitz-type inhibitor in murine renal cell carcinoma model. *Oncotarget.* 2016;7:62255–62266.
- [26] Chudzinski-Tavassi AM, Morais KL, Pacheco MT, et al. Tick salivary gland as potential natural source for the discovery of promising antitumor drug candidates. *Biomed Pharmacother.* 2016;77:14–19.
- [27] Branco VG, Iqbal A, Alvarez-Flores MP, et al. Amblyomin-X having a Kunitz-type homologous domain, is a noncompetitive inhibitor of FXa and induces anticoagulation in vitro and in vivo. *Biochim Biophys Acta.* 2016;1864:1428–1435.
- [28] Katia LP, Morais KFMP, Mario Thiego Fernandes Pacheco, Carolina Maria Berra, Miryam Paola Alvarez-Flores, and Ana Marisa Chudzinski-Tavassi. Rational development of a novel TFPI-like inhibitor from *Amblyomma cajennense* tick. *Toxin Rev.* 2013;33:48–52.
- [29] Maria DA, de Souza JG, Morais KL, et al. A novel proteasome inhibitor acting in mitochondrial dysfunction, ER stress and ROS production. *Invest New Drugs.* 2013;31:493–505.
- [30] Drewes CC, Dias RY, Branco VG, et al. Post-transcriptional control of Amblyomin-X on secretion of vascular endothelial growth factor and expression of adhesion molecules in endothelial cells. *Toxicol.* 2015;101:1–10.
- [31] Hembrough TA, Ruiz JF, Papatthanassiu AE, et al. Tissue factor pathway inhibitor inhibits endothelial cell proliferation via association with the very low density lipoprotein receptor. *J Biol Chem.* 2001;276:12241–12248.
- [32] Kobayashi H, Suzuki M, Kanayama N, et al. Suppression of urokinase receptor expression by bikunin is associated with inhibition of upstream targets of extracellular signal-regulated kinase-dependent cascade. *Eur J Biochem.* 2002;269:3945–3957.
- [33] Baranowska K, Misund K, Starheim KK, et al. Hydroxychloroquine potentiates carfilzomib toxicity towards myeloma cells. *Oncotarget.* 2016;7:70845–70856.
- [34] Hambley B, Caimi PF, William BM. Bortezomib for the treatment of mantle cell lymphoma: an update. *Ther Adv Hematol.* 2016;7:196–208.
- [35] Niewerth D, Kaspers GJ, Jansen G, et al. Proteasome subunit expression analysis and chemosensitivity in relapsed paediatric acute leukaemia patients receiving bortezomib-containing chemotherapy. *J Hematol Oncol.* 2016;9:82.
- [36] Castro TB, Hallack Neto AE, Atalla A, et al. Pharmacovigilance of patients with multiple myeloma being treated with bortezomib and/or thalidomide. *Braz J Med Biol Res = Revista brasileira de pesquisas medicas biologicas/Sociedade Brasileira de Biofisica [et al].* 2016;49:e5128.
- [37] Lu P, Takai K, Weaver VM, et al. Extracellular matrix degradation and remodeling in development and disease. *Cold Spring Harb Perspect Biol.* 2011;3:a005058.
- [38] Nagai S, Nakamura M, Yanai K, et al. Gli1 contributes to the invasiveness of pancreatic cancer through matrix metalloproteinase-9 activation. *Cancer Sci.* 2008;99:1377–1384.
- [39] Badgwell DB, Lu Z, Le K, et al. The tumor-suppressor gene ARHI (DIRAS3) suppresses ovarian cancer cell migration through inhibition of the Stat3 and FAK/Rho signaling pathways. *Oncogene.* 2012;31:68–79.
- [40] Batista IF, Ramos OH, Ventura JS, et al. A new Factor Xa inhibitor from *Amblyomma cajennense* with a unique domain composition. *Arch Biochem Biophys.* 2010;493:151–156.
- [41] Jaffe EA, Nachman RL, Becker CG, et al. Culture of human endothelial cells derived from umbilical veins. Identification by morphologic and immunologic criteria. *J Clin Invest.* 1973;52:2745–2756.
- [42] Toth M, Fridman R. Assessment of Gelatinases (MMP-2 and MMP-9) by Gelatin Zymography. *Methods Mol Med.* 2001;57:163–174.